Satellite Studies of Magnetospheric Substorms on August 15, 1968

9. Phenomenological Model for Substorms

R. L. McPherron,[1] C. T. Russell,[2] and M. P. Aubry[3]

In the eight preceding papers, two magnetospheric substorms on August 15, 1968, were studied with data derived from many sources. In this, the concluding paper, we attempt a synthesis of these observations, presenting a phenomenological model of the magnetospheric substorm. On the basis of our results for August 15, together with previous reports, we believe that the substorm sequence can be divided into three main phases: the growth phase, the expansion phase, and the recovery phase. Observations for each of the first three substorms on this day are organized according to this scheme. We present these observations as three distinct chronologies, which we then summarize as a phenomenological model. This model is consistent with most of our observations on August 15, as well as with most previous reports. In our interpretation we expand our phenomenological model, briefly described in several preceding papers. This model follows closely the theoretical ideas presented more quantitatively in recent papers by Coroniti and Kennel (1972*a*, *b*; 1973). A southward turning of the interplanetary magnetic field is accompanied by erosion of the dayside magnetosphere, flux transport to the geomagnetic tail, and thinning and inward motion of the plasma sheet. Our observations indicate, furthermore, that the expansion phase of substorms can originate near the inner edge of the plasma sheet as a consequence of rapid plasma sheet thinning. At this time a portion of the inner edge of the tail current is 'short circuited' through the ionosphere. This process is consistent with the formation of a neutral point in the near-tail region and its subsequent propagation tailward. However, the onset of the expansion phase of substorms is found to be far from a simple process. Expansion phases can be centered at local times far from midnight, can apparently be localized to one meridian, and can have multiple onsets centered at different local times. Such behavior indicates that, in comparing observations occurring in different substorms, careful note should be made of the localization and central meridian of each substorm.

In the preceding papers we have examined in detail many features of two magnetospheric substorms that occurred on August 15, 1968. We have chosen these substorms because of the near ideal location of the Ogo 5 spacecraft during this interval. Our main purpose in this study has been to establish the sequence of events that occurs during a single substorm, with the eventual goal of determining the mechanism responsible for triggering the onset of the expansion phase. Our primary emphasis has been changes in the configuration of the near-tail region.

In papers 1 and 4 we briefly outlined a speculative theoretical model of substorms to motivate our presentation of the data. This model is quite similar to that discussed in a more quantitative manner by *Coroniti and Kennel* [1972*a*, *b*, 1973]. Our primary purpose in this paper, the last in our sequence of papers, is to present a phenomenological model of substorms based on our observations discussed in the preceding papers. To do this, we first summarize our observations during the three substorms and then, in a separate section, describe this model, including brief references to the literature for facts not observed in this study. Our results indicate that the substorm expansion is triggered by thinning of the inner edge

[1] Department of Planetary and Space Science and Institute of Geophysics and Planetary Physics, University of California, Los Angeles, California 90024.

[2] Institute of Geophysics and Planetary Physics, University of California, Los Angeles, California 90024.

[3] Department of Planetary and Space Science, University of California, Los Angeles, California 90024. Now at Departement RSR, Centre National d'Etudes des Telecommunications, Issy-les-Moulineaux, France.

Copyright © 1973 by the American Geophysical Union.

of the plasma sheet to near zero thickness in a limited sector of local time. As will be discussed later, it is possible to resolve the present controversy with respect to the existence of a substorm growth phase in terms of this modified theoretical model.

As we show below, the satellite observations of substorms can be separated into two well-defined phases, the growth phase and the expansion phase. The expansion phase in space corresponds closely to that defined by ground observations, e.g., those of *Akasofu* [1968]. However, the growth phase, although quite clearly defined in space, is not readily apparent in ground observations, except for isolated substorms [*McPherron*, 1970]. Similarly, the recovery phase, apparently quite distinct in ground observations [*Akasofu*, 1968], is not readily distinguished from the expansion phase in the satellite observations. For our purposes in this paper we divide our phenomenological model into four parts, growth, expansion onset, expansion, and recovery, remembering that there are not necessarily distinct phases in all parts of the magnetosphere. In the next section we discuss each of these phases in turn for the three substorms.

Summary of Observations

To organize the many observations presented in previous papers, we have prepared tables presenting the sequence of events occurring in each substorm. The timing of these events has been determined from data with time resolution of 1–3 min. In general, errors due to time resolution are small in comparison with errors due to difficulties in identifying the same event at different locations. Each table is divided into four parts, corresponding to the growth phase, expansion onset, expansion phase, and recovery phase. Each entry in these tables shows the universal time of the beginning of the event, the spatial location of the observations, a brief description of the event, and a reference to the paper and figure in which the original data appeared. Each of the first three substorms of August 15, 1968, is discussed separately in the following subsections.

The 0220 UT substorm expansion. The first substorm expansion on August 15, 1968, began about 0220 UT. This substorm event was relatively clear in the ground data but hardly seen in the lobe of the tail near the midnight meridian. The event was difficult to time precisely, apparently as a consequence of multiple onsets and an unusual location of its center of activity. Examination of data presented in Figures 3 and 5 of paper 1 reveals that the largest magnetic disturbances occurred in the auroral zone at Fort Churchill and at midlatitude at Dallas and Tucson. This is borne out by the data displayed in Figure 1 of this paper. Here we have plotted as a function of local time the expansion phase changes in the X (north) and Y

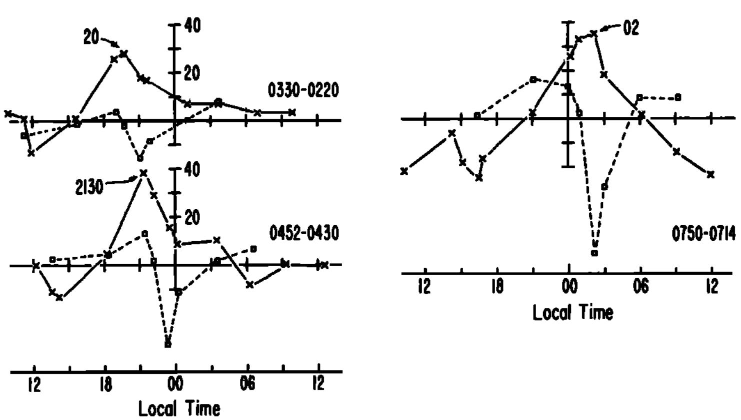

Fig. 1. The changes of the midlatitude magnetic field as a function of local time during the three substorm expansions on August 15, 1968. The X (north) component changes are indicated with a solid line. The Y (east) changes are indicated by a dashed line. The local time of the maximum disturbance is given on the plot for each substorm. These profiles should be compared with those shown in Figure 9 for a simple line current model.

TABLE 1. Chronological Events Occurring around the 0220 UT Substorm Expansion on August 15, 1968

Time, UT	Location	Event	Reference
		Growth Phase Phenomena	
0036	Midlatitude, U.S. sector	ΔH fluctuations, possibly responding to solar wind B_z fluctuations	Paper 1, Figure 5; paper 2, Figure 1
0150	Midlatitude, Dallas and Tucson	ΔH begins small temporary increase	Paper 1, Figure 5; paper 2, Figure 1
		Expansion Onset	
0205	Auroral zone, Great Whale	Beginning of small drop in H component; rapid field fluctuations begin	Paper 1, Figure 3
	Tail lobe, Ogo 5	B_z (GSM) begins 15-min increase changing sign at 0210	Paper 4, Figure 2
0210	Tail lobe, Ogo 5	B_y (GSM) begins small fluctuations causing changes in sign	Paper 4, Figures 2 and 3
0215	Auroral zone, Fort Churchill	X component begins sharp drop; field fluctuations begin	Paper 1, Figure 3
0218	Tail lobe, Ogo 5	Weak enhancement of ac electric field	Paper 8, Figure 1
0220	Midlatitude, Dallas and Tucson	ΔH begins large increase	Paper 1, Figure 5
0225	Auroral zone, Leirvogur	ΔH begins sharp drop	Paper 1, Figure 3
		Expansion Phase	
0228	Tail lobe, Ogo 5	First of two weak bursts of ULF waves	Paper 4, Figure 3
0230	Synchronous orbit, ATS 1	Sudden decrease in field magnitude; onset of turbulence	Paper 2, Figures 2 and 3
		Growth Phase Phenomena	
0237	Midlatitude, U.S. sector	ΔH begins to increase at San Juan and Fredericksburg; begins more rapid increase at Dallas	Paper 1, Figure 5
0242	Auroral zone, Great Whale	H component begins sharp drop with simultaneous sudden change in D	Paper 1, Figure 3; original data
0248	Auroral zone, Fort Churchill	X begins sharp drop	Paper 1, Figure 3
	Auroral zone, Baker Lake	Begin sharp negative bay	Paper 1, Figure 4
0306	Auroral zone, Great Whale	Begin negative bay	Paper 1, Figure 3
		Recovery Phase	
0310	Auroral zone, Baker Lake	Begin recovery of X component	Paper 1, Figure 4
0324	Auroral zone, Great Whale	Begin recovery of H component	Paper 1, Figure 3
0330	Midlatitudes, U.S. sector	End of increase in ΔH	Paper 1, Figure 5

(east) components at a worldwide chain of midlatitude magnetic observatories. The ordinates of these graphs were obtained by subtracting the X or Y magnetic field at the end of the expansion phase from that at the beginning. The expected quiet day variation during this interval was removed by using the variation observed on August 31, 1968. These profiles indicate the magnetic perturbation due to changes in the causative current systems associated with a substorm expansion [*Clauer et al.*, 1972]. The first panel of Figure 1 reveals that the central meridian of the 0220 UT substorm was near 2000 LT. The fact that this substorm is centered well before midnight is also readily apparent from visual analysis of the midlatitude magnetograms. From Table 1 we note that at 0215 UT there was a sudden drop in the X component and onset of rapid field fluctuations at Fort Churchill. At 0220 UT the H component at the midlatitude stations of Dallas and Tucson began to increase. Subsequently, as is shown in Table 1, there were a number of features both in the auroral zone and at midlatitudes that assure us that a substorm expansion actually occurred. As is indicated by the range of times shown for expansion onset (0205–0225), there is considerable uncertainty in the exact onset time.

The end of the expansion phase, i.e., the beginning of the recovery phase, occurred at the ground stations sometime between 0310 and 0330 UT. As we show below, this recovery phase was apparently obscured by the growth phase of a subsequent substorm.

It is apparent from Table 1 that this substorm provides no evidence of a substorm growth phase. Table entries at 0036 and 0150 UT indicate that, prior to the onset of the 0220 expansion, the solar wind magnetic field was fluctuating north and south. Similar fluctuations were seen at all midlatitude stations in the United States sector.

In summary, the sequence of events that occurred during this substorm was the following. For several hours the direction of the solar wind field fluctuated, remaining southward for short intervals of time. Auroral zone negative bays and midlatitude positive bays indicate that a substorm expansion resulted, beginning about 0220 and ending about 0330 UT. There is essentially no evidence of this substorm on the midnight meridian in the lobe of the tail. However, small changes in the dc field, small-amplitude ULF (magnetic), and VLF (electric) waves suggest that some event had occurred. A sudden decrease in the magnetic field and an onset of fluctuations at synchronous orbit in the late afternoon provide similar evidence.

The 0430 UT substorm expansion. The second substorm expansion on August 15, 1968, began almost precisely at 0430 UT. This onset was preceded by almost an hour of gradual changes throughout the magnetosphere. Some of these changes we consider evidence of a substorm growth phase, whereas others may be consequences of the preceding expansion. A chronological listing of the events in this substorm is presented in Table 2. We have tentatively assigned these events to four different intervals in a typical substorm sequence. The first noticeable event of this substorm was the sharp onset at 0318 UT of positive bays at auroral zone stations near the dusk meridian. Two minutes later the solar wind magnetic field on the dawn meridian at the moon reached a maximum northward value and began to decrease. Simultaneously there was the onset of a negative bay in the morning sector of the auroral zone and the beginning of an increase in the magnitude of the tail lobe field near the midnight meridian. By 0330 UT the cross-tail component of the magnetic field had begun to change in the tail lobe. Also at this time the H component at almost all midlatitude observatories began a nearly simultaneous decrease. At 0336 UT the field magnitude at synchronous orbit nearly on the dusk meridian began to decrease as well. At the moon on the dawn meridian the solar wind field became southward and remained this way for more than an hour.

We cannot definitely rule out the possibility that some of the above effects are consequences of the preceding expansion or associated with a new expansion around 0320 UT. There are several facts with which we can argue against these possibilities, however. To begin with, the first noticeable effects are delayed 1 hour with respect to the preceding expansion. This is almost twice the duration of a typical substorm expansion. Next, we note that many of the effects are nearly simultaneous throughout the magnetosphere rather than progressive as might be expected for a substorm expansion. Further, we note that magnetically there is little evidence of a substorm expansion near midnight at 0330 UT, despite the positive and negative bay onsets in the auroral zone at this time. In addition, the solar wind had been consistently northward during the preceding hour, whereas most isolated substorm expansions follow periods of southward interplanetary field. Finally, the response of the near tail lobe after 0330 UT is not consistent with the expected behavior during a substorm expansion.

From the preceding arguments we conclude that the observed effects after 0330 UT are probably consequences of a southward solar wind magnetic field and precursors of the later substorm expansion. We note in passing, however, that effects in the magnetosphere preceded by as much as 18 min the arrival of the southward field at the moon. To understand such a lengthy delay, we may argue that the solar wind discontinuity containing the change in field direction was tilted with respect to the solar wind velocity vector. If this were

TABLE 2. Chronological Events during the 0430 UT Substorm Expansion on August 15, 1968

Time, UT	Location	Event	Reference
		Growth Phase Phenomena	
0318	Auroral zone, College and Barrow	Begin sharp positive bay	Paper 1, Figure 3
0320	Moon, dawn, Explorer 35	Solar wind field begins to decrease from northward maximum	Paper 2, Figure 1
	Tail lobe, Ogo 5	Magnitude of tail field begins to increase	Paper 4, Figure 2
	Auroral zone, Leirvogur	Beginning of a negative bay in morning sector	Paper 1, Figure 3
0330	Midlatitude	H component begins to decrease almost everywhere nearly simultaneously	Paper 1, Figure 5
0330	Tail lobe, Ogo 5	B_y begins to increase changing sign at 0355	Paper 4, Figure 2
0336	Moon, dawn, Explorer 35	Solar wind field becomes southward	Paper 2, Figure 1
	Synchronous orbit, ATS 1	Begin decrease in field accompanied by fluctuations	
0413	Tail lobe, Ogo 5	B_z component is at minimum and begins slow increase	Paper 4, Figure 2
		Expansion Onset	
0420	Midlatitude, Fredericksburg	Begin slow increase in H component	Paper 1, Figure 5
0425	Tail lobe, Ogo 5	B_y reaches maximum positive value and begins to decrease	Paper 4, Figure 2
0428	Midlatitude, San Juan	Begin slow increase in H component	Paper 1, Figure 5
	Tail lobe, Ogo 5	Magnitude of tail field begins to decrease	Paper 4, Figure 2
0430	Auroral zone, Fort Churchill	Sudden onset of negative bay at Fort Churchill	Paper 1, Figure 3
0430	Auroral zone, Meanook	Sudden onset of transition bay at Meanook, current to north	Paper 1, Figure 3; original data
	Midlatitude, Dallas, Tucson	Begin increase in H component	Paper 1, Figure 5
0432	Synchronous orbit, ATS 1	H component begins rapid recovery to quiet level	Paper 2, Figures 2 and 3
	Tail lobe, Ogo 5	Sudden increase in flux of protons	Paper 5, Figure 1
0434	Auroral zone, Sitka	Sharp onset of positive bay, current north of Sitka	Paper 1, Figure 3; original data
		Expansion Phase	
0444	Tail lobe, Ogo 5	Field inclination begins rotation toward more dipolar configuration	Paper 4, Figure 3
0446	Auroral zone, Great Whale	Onset of large decrease in H, very short duration	Paper 1, Figure 3
	Auroral zone, Baker Lake	Begin negative bay at Baker Lake, current to south	Paper 1, Figure 4
	Tail lobe, Ogo 5	Weak enhancement of ac electric fields	Paper 8, Figure 1
0446	Tail lobe, Ogo 5	Beginning of 3 orders of magnitude increase in electron flux	Paper 5, Figure 2
0447	Midlatitude, Fredericksburg and San Juan	Begin sudden increase in H	Paper 1, Figure 5
0450	Tail lobe, Ogo 5	Inclination of field begins final rapid rotation	Paper 4, Figure 2
		Recovery Phase	
0450	Auroral zone, Great Whale	Begin recovery from negative bay in H	Paper 1, Figure 3
	Auroral zone, Meanook	Begin recovery of Z component	Original data
0452	Tail lobe, Ogo 5	ac electric fields reach maximum amplitude	Paper 8, Figure 1
0455	Auroral zone, Sitka	End of positive bay	Paper 1, Figure 3
0500	Auroral zone, Sitka	Begin recovery at Baker Lake, Leirvogur, and College	Paper 1, Figures 3 and 4
	Midlatitude, San Juan	End of H increase	Paper 1, Figure 5
0530	Synchronous orbit, ATS 1	End recovery in H component	Paper 2, Figure 3
0600	Auroral zone	All bays have recovered to quiet level	Paper 1, Figure 3

the case, the southward field might arrive at the earth considerably before it did at the moon. Alternatively, we may suggest that the important parameter in substorm occurrence is the angle of the solar wind field vector with respect to the GSM Z axis. Then any rotation of the field away from northward (decrease in B_z if magnitude constant) would increase the solar wind interaction with the magnetosphere.

The onset of the second substorm expansion is somewhat more clearly defined than the onset of the first. This expansion apparently began about 0420 UT near the midnight meridian with a slow increase in the H component at Fredericksburg. Five minutes later the Ogo 5 satellite in the tail lobe recorded the beginning of a rapid decrease in the cross-tail component of the field. At 0428 UT the H component at the midnight midlatitude station San Juan began to increase as simultaneously the magnitude of the tail lobe field began to decrease. At 0430 UT there were a number of large simultaneous changes both in the auroral zone and midlatitudes, which we attribute to the beginning of the expansion phase. In the auroral zone there were very sudden bay onsets at Fort Churchill and Meanook. At midlatitudes Dallas and Tucson began rapid increases in the H component. Examination of the ground data in paper 1, Figures 3 and 5, shows that the largest ground magnetic effects occurred at Fort Churchill and Tucson (see also Figure 1 of present paper). From the diagram in Figure 2 of paper 1 we find that these stations were located at about 2200 LT. At this local time Great Whale is located just before magnetic midnight (0530 UT) and for a typical substorm should have seen larger effects than Fort Churchill. Consequently, we conclude that the 0430 UT substorm expansion was centered at approximately 2200 LT. This is clearly substantiated by the midlatitude profiles of Figure 1. Within 2 min the field magnitude at synchronous orbit on the dusk meridian began to increase, and there was a sudden burst of energetic protons in the lobe of the tail. Four minutes after the expansion onset a positive bay began in the auroral zone at the dusk meridian.

From the preceding discussion we conclude that it may not be possible to precisely define the onset of an expansion phase for every substorm. Furthermore, the most pronounced effects of an expansion may occur at local times other than those at which the onset is first seen.

Continuing with our examination of the events summarized in Table 2 we find a number of effects throughout the magnetosphere that we attribute to the expansion phase of this substorm. At 0444 UT the direction of the lobe field temporarily rotated from a taillike configuration to a more dipolar configuration. Two minutes later both energetic electron and proton fluxes began a 3 orders of magnitude increase in the near tail. Simultaneously, there was a large enhancement in VLF electric field amplitudes. In the auroral zone there was a sudden onset of negative bays at midnight stations. Also, the midlatitude stations near midnight began a more rapid increase in H. Finally, at 0450 UT the tail field began a final rapid rotation toward a dipolar configuration.

In paper 4 we advanced a number of arguments that led us to the conclusion that, prior to 0444 UT, Ogo 5 was in the lobe of the tail. After this time we believe the appearance of particles, changes in field configurations, and ac electric and magnetic field fluctuations all indicate that the satellite was engulfed in an expanding plasma sheet. In paper 4 we also argued on a basis of timing and assumed plasma sheet expansion velocity of 10 km/sec that at 0430 the half-thickness of the plasma sheet was 0.9 R_E. Using values of 20 or 5 km/sec gave a half-thickness of 0.0 or 1.6 R_E.

From our preceding discussion of the details of expansion onset as observed from the ground it appears that this was a fairly complicated substorm. Possibly a very slow expansion began at 0420 UT on the midnight meridian. Ten minutes later a rapid expansion began on the 2200 LT meridian. Fifteen minutes later (still 0444 UT) the velocity of expansion increased on the midnight meridian, and simultaneously Ogo 5 was engulfed in the expanding plasma sheet. Possibly then different parts of the tail lobe and plasma sheet were undergoing quite different motions. If this is the case, our model of the substorm sequence requires considerably more sophistication to treat such substorms.

To conclude our discussion of this event, we summarize the recovery phase events presented in Table 2. Between 0450 and 0500 UT almost all stations in the auroral zone recorded their maximum deviations, both positive and negative. During this time the largest ac electric fields were recorded in the tail at Ogo 5. By 0600 UT almost all auroral zone stations had returned to more or less quiet time levels, although they remained somewhat disturbed. Similarly, the field at synchronous orbit completed its recovery between 0530 and 0600 UT.

The 0714 substorm expansion. The third substorm expansion on August 15, 1968, appears to have been an ideal event. Ground magnetic signatures of this event more closely approximate those of a 'typical' substorm than either of the preceding expansions. Similarly, the observed behavior in the tail corresponds closely to our theoretical model of substorm behavior. Fortunately, we also have the best collection of data describing this event, as is evident from the length of Table 3.

As is discussed in paper 4, the Ogo 5 satellite was near the midnight meridian and in the plasma sheet approximately 8 R_E behind the earth at the beginning of this event. As the growth phase progressed, the near plasma sheet thinned, and the satellite passed into the lobe of the tail. At the time this occurred, the satellite was so close to the expected position of the neutral sheet that the plasma sheet had to be less than 0.5 R_E in half-thickness for this to have occurred.

The evidence that this substorm had a significant growth phase is very strong, as can be seen from Table 3. At 0630 UT the solar wind magnetic field at the moon on the dawn meridian turned strongly southward for more than an hour. At the same time a negative bay began in the morning sector, and a positive bay began in the late afternoon sector. Ten minutes later the field at synchronous orbit about 3 hours past dusk began to decrease. Simultaneously, all midlatitude stations began a similar decrease. In the near plasma sheet the inclination of the cusp field began to increase, and its declination to decrease. Within several minutes the pitch angle distribution of progressively lower-energy electrons became isotropic. At 0646 UT the flux of low pitch angle electrons began to decrease, and at 0650 UT the spatial profile of energetic protons at Ogo 5 showed a significant reduction above the satellite. All electron fluxes were isotropic at this time. At 0653 UT smoothly varying electron precipitation began in the auroral zone at 2100 MLT (magnetic local time). Two minutes later the spatial profiles of energetic protons indicate that the boundary of the plasma sheet on the midnight meridian was thinning with the velocity of 4 km/sec. By 0659 UT a 'thinning wave' formed above Ogo 5. The spatial *e* folding parameter for this profile was 0.2 R_E above as compared to 0.6 R_E below the satellite. Two minutes later this thinning wave reached Ogo 5. At 0703 UT electron precipitation at 2100 MLT in the auroral zone was a maximum. At 0707 UT a number of phenomena were seen simultaneously at Ogo 5. The field magnitude began to increase rapidly while the declination decreased. Electron fluxes began a very rapid decrease. The average velocity of the plasma sheet over the interval 0640–0707 UT, estimated from electron flux profiles, was 10 km/sec. The spatial profiles of proton fluxes give a maximum boundary velocity at this time of 10 km/sec. By 0710 UT the boundary motion had ceased according to the proton observations. The *e* folding distance of the boundary at this time was 0.03 R_E. The half-thickness of the plasma sheet was of the order of 0.2–0.3 R_E. From all indications Ogo 5 was outside the plasma sheet. Its location was 7.7 R_E behind the earth, roughly 0.5 R_E above the expected neutral sheet.

The observations during the time interval 0640–0715 UT are consistent with our model of a substorm growth phase. Thus a southward solar wind magnetic field is followed by an increasingly taillike field in the cusp. During these changes the plasma sheet thins, as electrojet currents flow in the auroral zone, accompanied by low-level electron precipitation. We note that the bay onsets around 0640 UT are not accompanied by any sudden features characteristic of substorm expansions. Consequently, we associate the ionospheric currents and precipitation with the gradual changes of magnetic field configuration in the near tail.

The onset of the expansion phase of the third substorm is very precisely determined,

TABLE 3. Chronological Events during the 0714 UT Expansion on August 15, 1968

Time, UT	Location	Event	Reference
		Growth Phase	
0532	Dawn meridian, moon	Solar wind field turns sporadically southward for 40 min	Paper 2, Figure 1
0610	Dawn meridian, moon	Solar wind field turns northward for 20 min	Paper 2, Figure 1
0630	Dawn meridian, moon	Solar wind field turns southward for more than 1 hour	Paper 2, Figure 1
	Auroral zone	Beginning of negative bay at Great Whale; positive bays at College	Paper 1, Figure 3
0640	Auroral zone, Leirvogur	Begin weak negative bay	Paper 1, Figure 3
	Midlatitudes	Begin nearly simultaneous decrease in H component at nearly all stations	Paper 1, Figure 5
	Synchronous orbit, ATS 1	Begin quiet decrease in H component at 2040 LT	Paper 2, Figures 2 and 3
	Midnight, near plasma sheet	Begin gradual increase in field inclination and decrease in declination	Paper 4, Figure 3
0642	Midnight, near plasma sheet	Pitch angle distribution of 822-kev electrons becomes isotropic	Paper 6, text
0644	Midnight, near plasma sheet	Pitch angle distribution of 479-kev electrons becomes isotropic	Paper 6, text
0646	Midnight, near plasma sheet	Flux of electrons at low pitch angles begins to decrease	Paper 5, Figure 2
0650	Midnight, near plasma sheet	All electron energies become isotropic	Paper 5, Figure 2
0653	Auroral zone, Tungsten	Smoothly varying electron precipitation begins at 2100 MLT	Paper 2, Figure 4
0655	Midnight, near plasma sheet	East-west asymmetry in proton fluxes gives a plasma sheet thinning velocity of 4 km/sec	Paper 7, Figure 10
0659	Midnight, near plasma sheet	Thinning wave forms above Ogo 5 (0–2 R_E above; 0.6 R_E below)	Paper 7, Figures 8 and 9
0701	Midnight, near plasma sheet	Thinning wave reaches Ogo 5 according to proton fluxes	Paper 7, Figure 8
0703	Auroral zone, Tungsten	Electron precipitation maximum at 2100 MLT	Paper 2, Figure 4
0707	Midnight, near plasma sheet	Field magnitude begins to increase rapidly; declination decreases	Paper 4, Figure 3
	Midnight, near plasma sheet	Begin very rapid decrease in electron flux	Paper 5, Figure 2
	Midnight, near plasma sheet	Boundary velocity at maximum (10 km/sec) according to proton fluxes	Paper 7, Figure 10
	Midnight, near plasma sheet	Average plasma sheet thinning velocity 0655–0707 deduced from changes in electron flux profiles is 10 km/sec	Paper 5, text
0710	Midnight, near plasma sheet	No further evidence of boundary thinning in proton data; boundary scale 0.03 R_E; half-thickness $\sim$0.2–0.3 R_E	Paper 7, text
		Expansion Onset	
0712	Auroral zone	Sudden changes and onset of fluctuations at Meanook, Victoria, and College	Original data
0713	Near tail, lobe, Ogo 5	Begin very rapid increase in flux of electrons	Paper 5, Figure 2
0714	Moon, dawn meridian	Large fluctuation in B_y and B_z in solar wind	Paper 2, Figure 1
	Auroral zone	Begin trigger bay at Fort Churchill, D changes at Sitka	Paper 1, Figure 3 and original data
0714	Midlatitudes	Begin sharp increase at Dallas and Tucson	Paper 1, Figure 5
	Near tail, lobe, Ogo 5	Begin sudden decrease in field magnitude and inclination; also begin increase in declination, B_z, and rms power	Paper 4, Figure 3
0715	Auroral zone, Tungsten	Begin sudden burst of energetic electron precipitation (2100 MLT)	Paper 2, Figure 4

TABLE 3 (continued)

Time, UT	Location	Event	Reference
	Auroral zone, Tungsten	Auroral arcs begin to spread and become diffuse	Paper 2, text
	Midlatitudes	Begin large increase in D	Original data
		Expansion Phase	
0716	Near tail, plasma sheet	Plasma sheet boundary expanding at 90 ± 30 km/sec	Paper 7, text
0718	Synchronous orbit, ATS 1	Begin partial turbulent recovery of field magnitude	Paper 2, Figures 2 and 3
0720	Auroral zone, Tungsten	Westward surge passes overhead	Paper 2, text
0723	Auroral zone, Tungsten	Begin main bay at Fort Churchill	Paper 1, Figure 3
0725	Auroral zone, Tungsten	Begin bay effects at Baker Lake north of Fort Churchill	Paper 1, Figure 4
0727	Midlatitudes	Begin sharp increase at Fredericksburg (0200 LT)	Paper 1, Figure 5
0728	Auroral zone	Begin bay effects at Great Whale	Paper 1, Figure 3
0729	Near tail, plasma sheet, Ogo 5	Begin very strong ac electric fields at $3/2\,f_c$	Paper 8, Figure 1
	Near tail, plasma sheet, Ogo 5	Begin increase in field magnitude without rotation	Paper 4, Figure 3
0733	Auroral zone, Tungsten	Visual aurora to north	Paper 2, text
0734	Near tail, plasma sheet, Ogo 5	Begin rapid increase in transverse flux (betatron acceleration)	Paper 5, Figure 5
		Recovery Phase	
0742	Midlatitudes	End of increase in H component at midnight stations	Paper 1, Figure 5
0750	Auroral zone	Begin recovery at Baker Lake and Leirvogur	Paper 1, Figure 3
0750	Midlatitude	End increase in H at San Juan	Paper 1, Figure 5
0800	Auroral zone	Begin recovery at Meanook, Sitka, and College	Paper 1, Figure 3
0810	Auroral zone	Begin recovery at Great Whale	Paper 1, Figure 3

between 0712 and 0715 UT. The earliest observable effects were in the early evening sector of the auroral zone at Meanook, Sitka, and College. Within a minute the flux of energetic electrons began to increase at Ogo 5 on the midnight meridian. At 0714 UT a large fluctuation in B_Y and B_Z of the solar wind was observed at the moon on the dawn meridian. Simultaneously, in the auroral zone a trigger bay was observed at Fort Churchill (almost at magnetic midnight), and large declination changes were seen at Sitka. At midlatitude there was a sudden increase in H at the midnight stations. In the near tail the field magnitude and inclination began to decrease as the declination, B_Z, and rms power increased. One minute later there was a burst of energetic electron precipitation at 2100 MLT, whereas the arcs in visual aurora began to spread and became diffuse.

As the expansion phase continued, a variety of phenomena were seen throughout the magnetosphere. At 0716 UT estimates of the velocity of the expanding plasma sheet made with the proton observations give 90 ± 30 km/sec. Within 2 min the field at synchronous orbit (2100 LT) began a partial turbulent recovery. In the auroral zone at the same local time a westward-traveling surge passed over Tungsten, Northwest Territories, Canada. By 0723 UT the main bay began at Fort Churchill and bay effects were beginning to be noticed at Baker Lake, north of Fort Churchill. At 0727 UT the early morning (midlatitude) station (0200 LT) of Fredericksburg began its recovery, whereas, in the auroral zone, bay effects became noticeable at Great Whale (0130 MLT). At 0729 UT the magnitude of the field in the near tail began to increase without any associated rotation. Also at this time very strong ac electric fields at 3/2 the electron gyrofrequency began to be observed at Ogo 5. By 0733 UT visual aurora were to the north of Tungsten, and in the near tail there was a rapid increase in the flux electrons at large pitch angles. This increase occurred during an interval of rapidly increasing field magnitude.

From the preceding discussion it is clear that a classical substorm expansion occurred. The features of the visual aurora, i.e., sudden brightening, westward surge, and northward expansion, represent a typical auroral substorm. Magnetic disturbances, including a trigger bay, beginning of rapid fluctuations, and northward movement of the electrojet at midnight, as well as an indented positive bay in the early evening, are all features of a typical polar magnetic substorm. Similarly, the midlatitude magnetic disturbances of positive bays at midnight and negative bays at dusk (the inverse of the auroral zone) are expected midlatitude substorm signatures. We note, furthermore, that the largest magnetic disturbances at midlatitude occurred just after local midnight (see panel 3 of Figure 1). Thus this substorm is ideal in the sense it was nearly centered on the midnight meridian as well as having had all the classical features very clearly defined. In the near tail and also at synchronous orbit the magnetic field changed in the manner expected from previous reports of substorm expansions.

To conclude our discussion of this event, we note that the recovery phase of this substorm on the ground began about 0742 UT. At this time most of the midlatitude stations had reached a maximum in the *H* component. At 0750 UT the highest latitude and late morning stations in the auroral zone began to recover from their negative bays. By 0800 UT the remaining auroral stations at midnight and earlier were also recovering.

Following this substorm there is evidence in the ground and synchronous orbit data that another weak expansion occurred at 0815 UT. This event was apparently very localized near the midnight meridian. Another expansion occurred at 0910 UT. During this interval we have no data on the orientation of the solar wind magnetic field. However, from 0900 to about 1000 UT the solar wind was southward, as it had been at 0724 UT, when data transmission from Explorer 35 ended. The weak event at 0815 UT apparently did not relieve the stress in the near tail because the next event at 0910 UT was much larger in magnitude and spatial extent. Ground magnetic signatures of both these events were somewhat similar to those of the 0430 UT expansion inasmuch as they do not have the simple form exhibited by the 0714 UT expansion.

Phenomenological Model of Magnetospheric Substorms

The observations reported in the previous sections can be combined with previous reports to create a phenomenological model of a magnetospheric substorm. In its simplest form the sequence of events that occurs during an isolated substorm is the following. A southward component of solar wind is carried outward from the sun by a solar wind of constant dynamic pressure. The discontinuity, behind which the field points southward, encounters the subsolar magnetopause, and the growth phase begins with the onset of erosion [*Aubry et al.*, 1970; *Meng*, 1970; *Fairfield*, 1971]. Electric fields and magnetic perturbations appear in the polar cap [*Heppner et al.*, 1971; *Mozer*, 1971*b*]. About the same time the magnitude of the tail field in the lobes begins to increase as perturbations occur in the cross-tail component of the lobe field. In the auroral zone, weak bays begin to develop, and westward electric fields [*Mozer*, 1971*a*] begin to appear. At synchronous orbit premidnight the field magnitude begins to decrease as similar variations occur on the surface at midlatitudes. In the near tail the plasma sheet begins to thin as the magnitude of the field begins to increase and rotate toward a more taillike configuration. In the auroral zone, weak electron precipitation begins. As the growth phase continues the near plasma sheet thins, progressively larger velocities and steepening particle gradients forming its boundary.

The expansion phase begins as the near-earth plasma sheet reaches nearly zero thickness. With near simultaneity an intense negative bay appears in the midnight sector of the auroral zone in conjunction with an intense southward electric field [*Mozer*, 1971*a*]. Rapid changes occur in the cross-tail component of the magnetic field as the plasma sheet begins to expand at approximately 10 times its thinning velocity. Inside the expanding plasma sheet, large-amplitude magnetic fluctuations accompany the sudden appearance of energetic particles. In the auroral zone the electrojet expands northward and westward in conjunction with intense electron precipitation. In the evening sector, positive bays are developing, whereas at midlatitudes the field becomes depressed. In the lobe of the tail the field magnitude begins to decrease. Eventually, with a delay dependent on distance above the neutral sheet, a portion of the lobe field is transformed into a more dipolar configuration by the expanding plasma sheet. Inside the plasma sheet the field magnitude begins to increase without corresponding rotations, and energization of electrons at large pitch angle occurs.

As the particle pitch angle distributions change, there are rapid changes in the type of high-frequency waves present. These waves are of sufficient strength and proper frequencies to cause pitch angle scattering and energization, further altering the particle distribution functions.

After approximately 30 min, ground magnetic records indicate that electrojet currents begin to decay and the recovery phase is in progress. The distant magnetic field slowly returns to a quiet time configuration.

INTERPRETATION

Our interpretation of the sequence of events that occurs during a magnetospheric substorm is in general agreement with the theoretical ideas presented in a recent series of papers by *Coroniti and Kennel* [1972*a*, *b*, 1973]. To show the consistency of our observations with these theoretical ideas, we present here a qualitative review of their theoretical model.

An approximate scale drawing of the magnetosphere in a symmetric configuration at equinox is presented in Figure 2. In this figure we identify the various regions playing important parts in the substorm process. As is apparent from the drawing, it is assumed that a southward solar wind magnetic field is responsible for magnetic merging. Merged lines are carried around the earth by the solar wind, eventually drifting across the lobe of the tail to a second merging region some distance behind the earth. The neutral line associated with this second merging region is assumed to define the outer boundary of the plasma sheet. Plasma

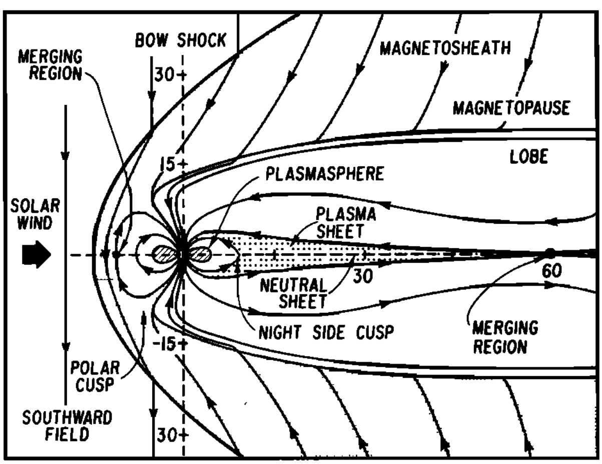

Fig. 2. A schematic view approximately to scale of the magnetosphere in the noon-midnight meridian plane. It is assumed that magnetospheric convection across the polar cap is driven by merging of a southward solar wind magnetic field, with the earth's dipole field. Convection toward the earth is driven by reconnection in a distant merging region. Major boundaries and regions that play a role in substorm behavior include the bow shock, the magnetosheath, the magnetopause, the polar cusps, the lobes of the tail, the plasma sheet, the neutral sheet, the nightside cusp, and the plasmasphere. The actual location of the distant merging region is unknown, and so it has been arbitrarily placed at the orbit of the moon.

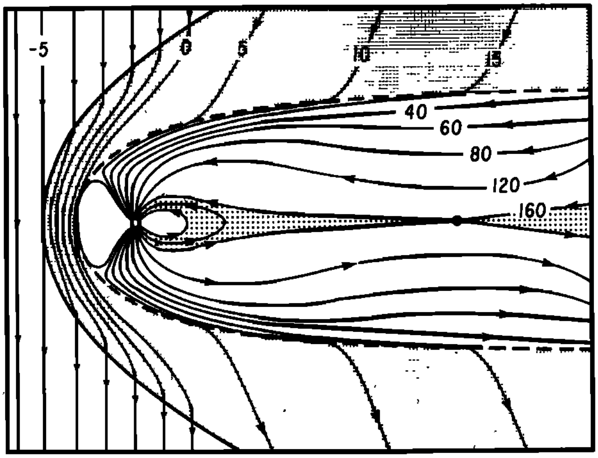

Fig. 3. An idealized picture of magnetospheric convection driven across the polar cap in the noon-midnight meridian plane by magnetic merging. The solar wind magnetic field is assumed entirely southward and flowing away from the sun at 5 R_E/min. Field lines are labeled in minutes, with the assumption that the feet of the field line are moving at a velocity determined by a 50-kev potential drop across the polar cap. The distant neutral line where reconnection occurs is arbitrarily placed at 60 R_E. The plasma sheet is bounded by the last closed field line passing through the neutral region.

ejected from the neutral line is convected toward the earth. Precipitation into the auroral oval creates a sharp inner boundary to the plasma sheet in the nightside cusp [*Kennel*, 1969].

The configuration of a given merged field line at successive times is shown in Figure 3. At $T = -5$ min a southward-pointing interplanetary field line encounters the bow shock. Five minutes later ($T = 0$) it enters the merging region at the subsolar point. As time progresses, the field line is rapidly swept back in the magnetosheath while its foot moves slowly across the polar cap creating polar cap electric fields and magnetic disturbances. Field lines are labeled at times determined by placing a 50-kev potential drop across a 30° sector centered on the north magnetic pole.

The changes in the quiet time magnetic field configuration that occur as a consequence of merging are shown in Figure 4. The boundary of the magnetopause moves inward as flux is eroded from the dayside. This flux is transported by the solar wind and added to the tail. However, because the dayside cross section of the magnetosphere has been reduced, the increased magnetic flux in the tail passes through a smaller cross section. Thus, as time progresses, there is a rapid increase in the magnitude of the tail field. At the same time the plasma sheet begins to thin. Also, because the solar wind drag on the magnetosphere has increased due to the merging, the earth must pull harder on the tail to balance forces [*Siscoe and Cummings*, 1969]. The force of the earth on the tail is the product of the gradient of the tail field at the center of the earth times the earth's dipole moment. Thus the solar wind drag can be balanced both by the strengthening of the tail currents and by the inward motion of the tail current system. In practice both occur. This, in turn, causes the field in the near-tail region to become increasingly taillike, and simultaneously it decreases the field closer to the earth at synchronous orbit.

Field-aligned currents should flow into the ionosphere as a result of convection, as is indicated schematically in Figure 5. In the right panel we show the electrostatic potential associated with convection and, for a single L shell, the approximate distribution of currents flowing to the ionosphere. Similar distributions flow on other L shells as well, so that the actual distribution is a volume current into the ionosphere postmidnight and a similar volume current out premidnight. These field-aligned currents produce changes in the cross-tail com-

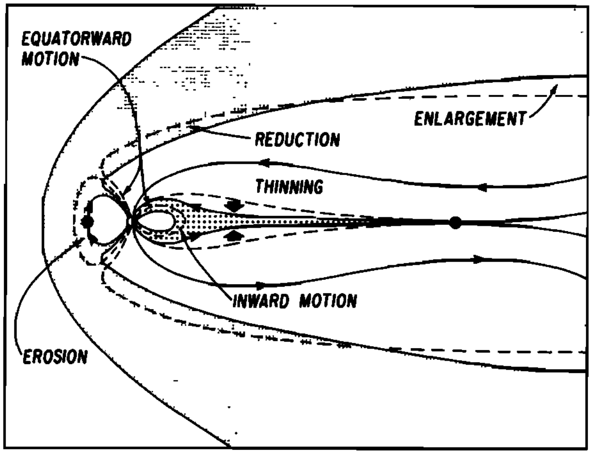

Fig. 4. Schematic diagram illustrating the major changes in magnetic field configuration that occur during the substorm growth phase. Erosion on the dayside moves the magnetopause earthward, reducing the front side cross section and moving the feet of the polar cusp field lines equatorward. Flux eroded from the dayside is convected to the tail, increasing the field magnitude in the near-earth region, because of the increased flux in a smaller cross section. Electric fields resulting from convection cause the plasma sheet to thin and the inner edge of the tail current to move earthward, projecting as an equatorward motion of nightside auroral arcs.

ponent of the near-tail field as well as changes in declination at ground magnetic observatories.

Also shown in the left panel of Figure 5 are the ionospheric currents expected as a result of the preceding field-aligned currents. These include the westward electrojet and poleward Hall currents. In this diagram we schematically indicate the volume field aligned

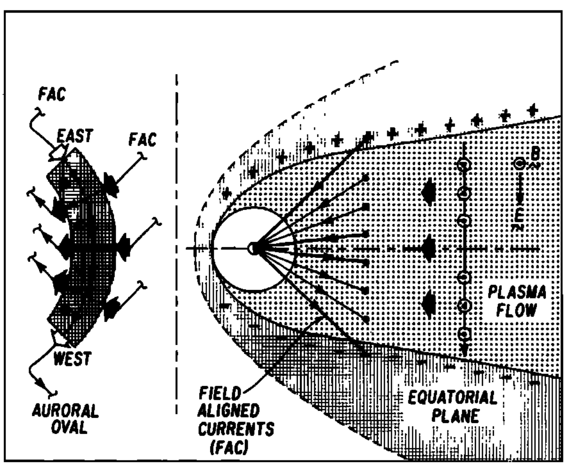

Fig. 5. Schematic representation of field-aligned and ionospheric currents that may flow near the midnight meridian as a consequence of earthward convection of plasma in the tail. In the right panel of the figure, polarization of the convecting plasma produces an electrostatic potential across the tail with positive space charge near the dawn side and negative space charge near the dusk. Equipotential field lines act as perfect conductors applying this potential to the ionosphere as shown for a given L shell in the diagram. This potential drives a westward Pedersen current in the auroral oval shown at the left of the figure. Poleward Hall currents are divergent at the boundaries of the highly conducting auroral oval. These divergent currents close via sheets of field-aligned currents.

currents (FAC) as lines entering the eastern end of the auroral oval and leaving the western end. If the boundaries of the auroral oval are defined by a high contrast in terms of ionospheric conductivity, sheets of field-aligned currents may close the poleward Hall currents through the magnetosphere. These sheets should flow near the inner and outer boundaries of the plasma sheet as defined in the discussion of Figure 2.

If the foregoing model of the growth phase is to explain our substorm observations on August 15, 1968, we must make some assumptions about the way in which the plasma sheet thins. These assumptions are illustrated in the scale drawing of Figure 6. In the top panel we show the quiet time configuration of the near tail at the beginning of the 0430 and 0714 UT growth phases. Vectors show the local field orientation at specific points on the Ogo 5 trajectory. In the 0430 UT substorm the satellite was initially in the north tail lobe just above the plasma sheet. In the 0714 UT substorm it was inside the plasma sheet near its inner edge.

The second panel shows the possible configuration about the middle of the growth phase. In the 0430 UT substorm more rapid thinning close to the earth, combined with a flaring tail cross section of the tail, created a lobe field with increased magnitude and negative Z components. In the 0714 UT substorm, inward motion of that tail current created a more taillike field in the nightside cusp region.

Finally, in the bottom panel we show the configuration slightly before the onset of the expansion phase. The tail current has moved close to the earth, and the plasma sheet at 8 R_E has become very thin. In fact, several minutes later the plasma sheet thins still more, and Ogo 5 passes outward into the lobe.

According to the theoretical model of *Coroniti and Kennel* [1972a] shown schematically in Figure 7 the onset of the expansion phase is the result of turbulent resistivity. They suggest that the field-aligned sheets of current flowing on the equatorward edge of the auroral oval become unstable. The current instability creates a large potential drop along field lines and allows the ionospheric Hall currents to build up on the boundary of the auroral oval.

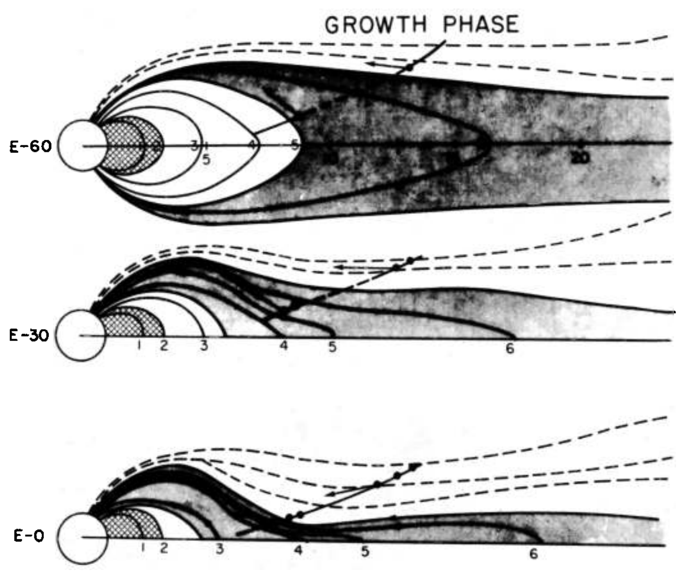

Fig. 6. Schematic drawing illustrating changes in the near geomagnetic tail during the 0430 and 0714 UT substorm expansions on August 15, 1968. The trajectory of the Ogo 5 satellite is shown by a heavy line descending out of the north lobe of the tail. Magnetic field observations at critical times in each substorm are shown by vectors at dots along the trajectory. The three panels summarize changes in the field configuration and structure of the plasma sheet inferred from the data.

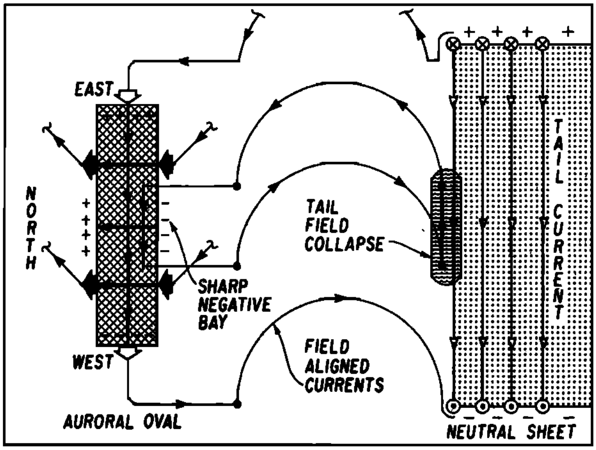

Fig. 7. Schematic illustration of the effects of disruption of the sheets of field-aligned currents that are closing poleward ionospheric Hall currents near midnight. Disruption of currents allows the auroral oval to polarize with an equatorward electric field. Westward Hall currents driven by this field add to the Pedersen current in the limited region of polarization. This additional current is divergent in the ionosphere and closes via field-aligned currents and an eastward cross-tail current. This eastward current in the tail is opposite to the tail current and just the perturbation needed to cause the collapse of the tail field. The net result is that the earthward portion of the tail current is diverted through the ionosphere, creating an intense westward electrojet of limited spatial extent.

A strong polarization electric field develops in a portion of the auroral oval driving an intense westward Hall current. To complete the circuit, field-aligned currents must flow into the ionosphere at the east and out at the west of the polarized region. If the east and west boundaries of the region of polarization are sufficiently sharp, the field-aligned currents connected to the westward Hall current will be well approximated by line currents. The magnetospheric closure of this system is an eastward equatorial current counter to the tail current. In actual fact there will be no real eastward current. Instead, as is shown by Figure 8, the cross-tail current is disrupted and 'short circuited' through the ionosphere.

We point out that the equatorial ionospheric electric field across the auroral oval in this model is a result of disruption of field-aligned sheets of current. In the *Coroniti and Kennel* [1972*a*] model this disruption occurs in the upper ionosphere. It is an equally likely possibility, however, that the disruption occurs in the magnetosphere. For example, as is suggested by Figure 6, an instability may develop in the near plasma sheet as a consequence of rapid thinning.

Regardless of the true nature of the physical mechanism causing the shorting out effect, this model can explain many of the observations summarized in our phenomenological model. At the onset of the expansion phase an intense westward electrojet flows in a limited sector of local time [*Akasofu*, 1968]. This electrojet is associated with an intense equatorward electric field [*Mozer*, 1971*a*; *Wescott et al.*, 1969]. Midlatitude positive bays during the expansion phase can be explained by the field-aligned currents driving the localized westward electrojet [*Meng and Akasofu*, 1969; *Akasofu and Meng*, 1969; *Bonnevier et al.*, 1970; *Fukushima*, 1969; *Crooker and McPherron*, 1972]. For example, Figure 9 shows a simple line current model of a substorm expansion discussed in a recent report by *Horning et al.* [1972]. Midlatitude magnetic profiles of the X (north) and Y (east) components of the field are in good agreement with the observations summarized in Figure 1. Finally, the disruption of the tail current causes a local collapse of the tail field to a more dipolar configuration.

As time progresses, the region of short-circuited tail current expands westward across the tail as well as away from the earth. These

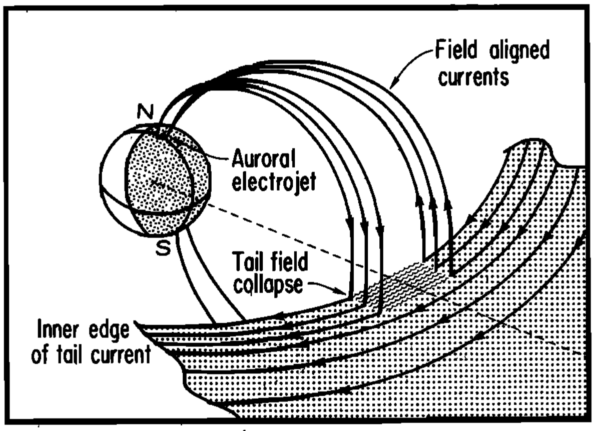

Fig. 8. A perspective drawing of the events described in Figure 7.

features are projected to the ionosphere as the northward expansion and the westward surge. As more current appears in the ionosphere, the surface magnetic effects increase in magnitude while simultaneously the near-tail region becomes more dipolar. Combined effects of the field-aligned currents and the disappearance of the inner edge of the tail current cause an increase in field at synchronous orbit.

Since the actual cause of the expansion phase is not known, we can only speculate about the way in which the plasma sheet expands. It seems likely from the observed velocities of expansion that the process is not the inverse of thinning, i.e., electric field drift. A possibility, consistent with the observations in these papers in the near tail and with measurements taken further down the tail with the Imp and Vela spacecraft, is that a neutral point forms in the near tail. Eventually, this point propagates away from the earth, followed by an expanding plasma sheet like the wake of a boat. The magnetic energy stored in the local field is converted to particle energy. The electric fields associated with the rapid field collapse cause further energization and radial injection of newly energized particles.

The preceding picture can account for the observed time delays in the arrival of the expansion phase effects at progressively higher locations in the tail [*Hones et al.*, 1970] and is consistent with the velocities obtained with multisatellite studies [*Akasofu et al.*, 1970; *Meng et al.*, 1970].

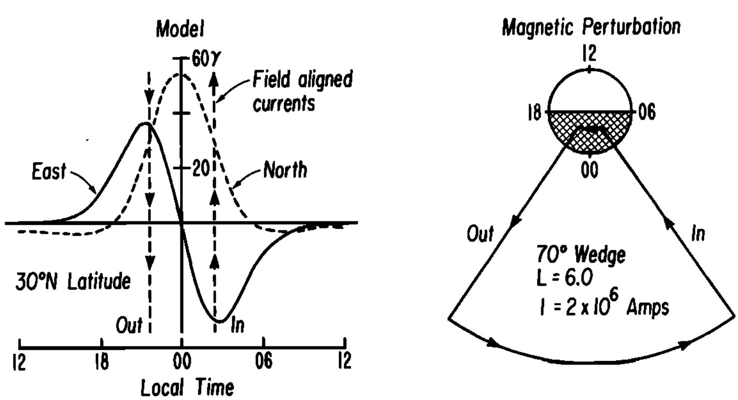

Fig. 9. A simple line current model in a dipole field of the expansion phase current system described in Figures 7 and 8. The right panel summarizes the model parameters, and the left panel the calculated midlatitude magnetic signature.

Discussion

The theoretical model presented schematically in the previous section is highly qualitative. Furthermore, not all observations are explained by this simple picture. We believe that this model is appropriate for isolated substorms and perhaps occasionally for specific ideal substorms in the middle of a sequence of substorms. In this section we discuss possible causes of the inconsistency of the observations with this model.

The basic elements of the proposed model of the growth phase are magnetic merging, solar wind flux transport, intermediate storage of magnetic energy in the tail lobes, reconnection of field, and inward convection and development of a near-earth tail current or partial ring current. For the expansion phase the basic elements are rapid thinning of a portion of the near-earth plasma sheet, disruption of the cross-tail current, polarization of the auroral oval, an intense westward electrojet connected via field-aligned currents to the tail current, and rapid outward expansion of the region of the disrupted tail current.

In this model the inner region of the tail current system is the immediate reservoir of energy during a substorm expansion. We note that a single expansion need only involve a portion of this reservoir. After a prolonged interval of northward interplanetary magnetic field and its associated period of little convection and magnetic quiescence, this reservoir of energy may be quite empty and require a lengthy growth phase to fill. In fact, examination of the evidence in the literature purporting to show the existence of a growth phase shows the least disputable cases to be either isolated events or the first in a sequence of substorms.

Once the inner reservoir of energy has been filled, we see no reason why several substorm expansions could not occur, even in the absence of further flux transport from the dayside. Such occurrences could explain occasional reports of substorm expansions during intervals of northward field. Also they could explain substorms that occur without buildup in the magnitude of the tail field, such as the 0220 UT expansion.

Since a substorm expansion may involve only a limited sector of the inner edge of the tail current, we see no obvious reason why a second expansion could not occur in some other sector. In general, if the first event persists, the two regions should eventually merge, and the resulting substorm would be described as a multiple-onset event. For example, this may have been the situation during the 0430 UT expansion. It may in fact be possible for an expansion phase to occur at one local time when a growth phase is in progress elsewhere. Under these circumstances it may be impossible to separate unambiguously the effects that are due to the expansion phase and those that are due to the growth phase. Finally, we note that during intervals of prolonged southward field it is likely that the tail field would become more or less steadily enhanced. Earthward convection would be continuous. Expansions might occur in different local time sectors with apparently random phase relations. Observations in the tail lobe and more distant plasma sheet might not be simply related to the near-earth and auroral zone phenomena.

Conclusions

Observations made during three substorms on August 15, 1968, are consistent with existing theoretical ideas about the cause of substorms. These observations are most simply organized by a phenomenological model consisting of three phases, a growth phase, an expansion phase, and a recovery phase. The growth phase includes solar wind erosion of the dayside magnetopause, solar wind transport of eroded flux to the tail, inward convection of plasma, establishment of an inward extension of the tail current or partial ring current, thinning of the plasma sheet, and field-aligned and ionospheric currents. The expansion phase includes the sudden appearance of an intense westward electrojet in a localized sector, a simultaneous collapse of the taillike field, the energization and injection of particles close to the earth, and rapid expansion of the plasma sheet boundaries into the lobes of the tail. The recovery phase is most apparent in the auroral zone and includes mainly the decay of the electrojet currents and the reestablishment of the quiet time auroral displays.

Our model of the expansion phase involves a disruption of the near tail. We propose that this occurs when the plasma sheet in a localized sector close to the earth becomes exceedingly thin. A neutral point formation and the subsequent motion into the far tail are consistent with our data and those of others. During disturbed times, different local time sectors can apparently become decoupled from each other and from the more distant tail, resulting in exceedingly complex substorm behavior.

As a result of these conclusions we suggest that future studies of substorms treat separately isolated substorms, the first substorm in a sequence, and substorms during disturbed intervals. We also suggest that it is important to distinguish between substorms with simple onsets and those with multiple onsets. In addition, it is important to specify the central meridian of a given substorm and the location of the observations relative to this meridian. To pursue such studies adequately requires complete longitudinal chains of ground-based magnetic observatories at low latitudes and in the auroral zone, complemented by one or more latitudinal chains of stations.

Acknowledgments. We acknowledge the many discussions of the meaning of the diverse data with our co-workers. We particularly thank those who finished their work early and remained patient while we attempted our synthesis of the final results. Our work on this phase of the project was supported by the National Aeronautics and Space Administration under research grant NGR 05-007-004. One of us (M.A.) was also supported by an ESRO-NASA fellowship.

* * *

Associate Editors L. J. Lanzerotti and G. C. Reid thank Referees R. L. Arnoldy, J. L. Burch, T. E. Holzer, E. W. Hones, Jr., N. C. Maynard, and T. J. Rosenberg for their assistance in evaluating this series of papers.

REFERENCES

Akasofu, S.-I., *Polar and Magnetospheric Substorms*, Springer, New York, 1968.

Akasofu, S.-I., and C.-I. Meng, A study of polar magnetic substorms, *J. Geophys. Res.*, *74*, 293, 1969.

Akasofu, S.-I., E. W. Hones, Jr., and C.-I. Meng, Simultaneous observations of an energetic electron event in the magnetotail by the Vela 3A and Imp 3 satellites, 2, *J. Geophys. Res.*, *75*, 7296, 1970.

Aubry, M. P., C. T. Russell, and M. G. Kivelson, Inward motion of the magnetopause before a substorm, *J. Geophys. Res.*, *75*, 7018, 1970.

Bonnevier, B., R. Bostrom, and G. Rostoker, A three-dimensional model current system for polar magnetic substorms, *J. Geophys. Res.*, *75*, 107, 1970.

Clauer, C. R., R. L. McPherron, B. L. Horning, and N. E. Cline, Midlatitude magnetic maps of disturbances due to magnetospheric substorms (abstract), *Eos Trans. AGU*, *53*(11), 1098, 1972.

Coroniti, F. V., and C. F. Kennel, Polarization of the auroral electrojet, *J. Geophys. Res.*, *77*, 2835, 1972*a*.

Coroniti, F. V., and C. F. Kennel, Changes in magnetospheric configuration during the substorm growth phase, *J. Geophys. Res.*, *77*, 3361, 1972*b*.

Coroniti, F. V., and C. F. Kennel, Can ionospheric line tying inhibit magnetospheric convection?, *J. Geophys. Res.*, *78*, in press, 1973.

Crooker, N. U., and R. L. McPherron, On the distinction between the auroral electrojet and partial ring current systems, *J. Geophys. Res.*, *77*, 6886, 1972.

Fairfield, D. H., Average and unusual locations of the earth's magnetopause and bow shock, *J. Geophys. Res.*, *76*, 6700, 1971.

Fukushima, N., Equivalence in ground geomagnetic effect of Chapman-Vestine's and Birkeland-Alfven's electric current systems for polar magnetic storms, *Rep. Ionos. Space Res. Japan*, *23*, 219, 1969.

Heppner, J. P., J. D. Stolarik, and E. M. Wescott, Electric-field measurements and the identification of currents causing magnetic disturbances of the polar cap, *J. Geophys. Res.*, *76*, 6028, 1971.

Hones, E. W., Jr., S.-I. Akasofu, P. Perreault, S. J. Bame, and S. Singer, Poleward expansion of the auroral oval and associated phenomena in the magnetotail during auroral substorms, 1, *J. Geophys. Res.*, *75*, 7060, 1970.

Horning, B. L., R. L. McPherron, and D. D. Jackson, An application of the linear inverse theory to parameterization of substorm field-aligned current models (abstract), *Eos Trans. AGU*, *53*, 1097, 1972.

Kennel, C. F., Consequences of a magnetospheric plasma, *Rev. Geophys. Space Phys.*, *7*, 379, 1969.

McPherron, R. L., Growth phase of magnetospheric substorms, *J. Geophys. Res.*, *75*, 5592, 1970.

Meng, C.-I., Variation of the magnetopause position with substorm activity, *J. Geophys. Res.*, *75*, 3252, 1970.

Meng, C.-I., and S.-I. Akasofu, A study of polar magnetic substorms, *J. Geophys. Res.*, *74*, 4035, 1969.

Meng, C.-I., E. W. Hones, Jr., and S.-I. Akasofu, Simultaneous observations of an energetic electron event in the magnetotail by Vela 3A and Imp 3 satellites, 1, *J. Geophys. Res.*, *75*, 7294, 1970.

Mozer, F. S., Origin and effects of electric fields during isolated magnetospheric substorms, *J. Geophys. Res.*, *76*, 7595, 1971*a*.

Mozer, F. S., Properties of polar cap electric fields (abstract), *Eos Trans. AGU, 52,* 904, 1971*b*.

Siscoe, G. L., and W. D. Cummings, On the cause of geomagnetic bays, *Planet. Space Sci., 17,* 1795, 1969.

Wescott, E. M., J. D. Stolarik, and J. P. Heppner, Electric fields in the vicinity of auroral forms from motions of barium vapor releases, *J. Geophys. Res., 74,* 3469, 1969.

(Received March 17, 1972;
accepted January 5, 1973.)